

AD No. 22 245
ASTIA FILE COPY

UNCLASSIFIED

TECHNICAL REPORT 2

**THE CRYSTAL STRUCTURE OF
BERTHIERITE, FeSb_2S_4**

M.J. Buerger and Theodor Hahn

**Office of Naval Research
Project NR 032 346
Contract N5ori-07860**

Massachusetts Institute of Technology

30 November 1953

<u>DISTRIBUTION LIST</u>	<u>No. Of Copies</u>
Chief of Naval Research, Washington, D.C.	2
Director, Office of Naval Research, Boston	1
Director, Office of Naval Research, New York	1
Director, Office of Naval Research, Chicago	1
Director, Office of Naval Research, San Francisco	1
Director, Office of Naval Research, Pasadena	1
Asst. Naval Attaché for Research, O.N.R., New York	2
Armed Services Tech. Information Agency, Dayton	5
Director, Naval Research Lab., Washington (TIO)	6
Office of Tech. Services, Dept. Commerce, Washington	1
Director, Naval Research Lab., Washington (Code 3500)	1
Bureau of Aeronautics, Dept. of Navy, Washington Attention: H.E. Promisel, AE-41 Mrs. Galane EL 4113	3 5
C.O., Naval Air Material Center, Philadelphia	1
Bureau of Ordnance, Dept. of Navy, Washington Attn: Rex, Tech. Library, Ad3	3 1
C.O., U.S. Naval Ordnance Test Station, Inyokern	1
Chief of Staff, U.S. Army, Washington	1
C.O., U.S. Naval Ordnance Lab., White Oaks	1
Office of Chief of Ordnance, Dept. of Army, Washington	3
Office of Chief of Engineers, Dept. of Army, Washington	1
Wright Air Development Center, W-P Air Force Base, Dayton	1
C.O., Office of Ordnance Research, Durham	1
Atomic Energy Commission, Metall. Branch, Washington	1
Nat. Advisory Com. for Aeronautics, Washington	1
Los Alamos Scientific Lab., Los Alamos	1
Sandia Corporation, Albuquerque	1

The Crystal Structure of
Berthierite, FeSb_2S_4

by M.J. Buerger and Theodor Hahn

Crystallographic Laboratory, Department of Geology and Geophysics,
Massachusetts Institute of Technology

Abstract

The general arrangement of atoms in berthierite had been suggested in an earlier publication by solving the Patterson function $P(\underline{x}\underline{y})$, with the aid of the minimum function $M_g(\underline{x}\underline{y})$. In this paper a report is given of the refinement of the structure. The intensities were measured by the M.I.T. modification of the Dawton method, and the resulting F^2 's were placed on an absolute basis by Wilson's method. The structure was refined by the use of successive differential Fourier syntheses. The final structure has a small residual factor and neatly reproduces the Patterson projection.

In the structure of berthierite each Sb atom is evidently bonded to 3 S atoms at distances of about 2.5°\AA . These SbS_3 groups share S atoms to form two non-equivalent SbS_2 chains parallel to the c axis. The Fe atoms are surrounded by 6 S atoms in approximately octahedral arrangement at distances of about 2.5°\AA . This is about the expected distance for ionic Fe-S bonds. The structure can therefore probably be regarded as $\text{Fe}^{++}(\text{SbS}_2)_2^-$.

Introduction

Material. The berthierite from Kisbanya, Carpathians, has been described in detail by Zsivny and Zombory (1934). These investigators were kind enough to make a generous sample of this material available for this crystal-structure investigation. The analysis of the Kisbanya berthierite indicates that it has almost exactly the ideal composition FeSb_2S_4 .

Unit cell and space group. The unit cell and space group of berthierite have been reported in an earlier communication (Buerger, 1936). The cell has the following dimensions:

$$\underline{a} = 11.44 \text{ \AA}^0$$

$$\underline{b} = 14.12$$

$$\underline{c} = 3.76$$

This cell contains $4\text{FeSb}_2\text{S}_4$. The space group is Pnam.

Intensity determination. The structure determination reported here was based upon hk0 and h0l reflections as recorded on precession photographs. The intensities were determined by using the M.I.T. modification of the Dawton (1938) method. The intensities were corrected for Lorentz and polarization factors, but no allowance was made for absorption.

In the course of the structure determination it became evident that the F values determined in this manner

were accurate and quite satisfactory except that there is a critical lower intensity below which one cannot distinguish a non-zero intensity from zero intensity. The lack of knowledge of the F 's having amplitudes between zero and the lowest observable amplitude was keenly felt as the refinement progressed.

Approximate locations of atoms

Rough intensity considerations had already shown that all atoms of berthierite were confined to the (001) reflection planes, that is, to equipoint 4c, for which $z = \pm \frac{1}{4}$. With the aid of the F_{hk0}^2 's, a Patterson projection $P(xy)$ was prepared, Fig. 1. In another place (Buerger, 1951) it was shown that this projection could be solved for the xy coordinates of the atoms by applying the minimum function (Buerger, 1950). The approximate electron density found by this method is shown in Fig. 2. The several dense areas, in order of decreasing density, are evidently the two antimony atoms, the one iron atom, and the four sulfur atoms. The close relation of this minimum function map to the true structure can be appreciated by comparing it with Fig. 3, the electron density projection $\rho(xy)$, as determined after refinement.

There is an interesting peculiarity about an approximate structure determined by image-seeking method:

One must make a decision regarding the location of at least the first image point. The location of the one atom corresponding to this image point is fixed by this choice and does not change in the course of applying the image-seeking function to find the other atoms of the structure. There is usually a small error involved in selecting an image point. For example, an error arises when the Patterson peak chosen for the image point is not a single peak, but rather the coalescence of several peaks not in exactly the same location. At this stage of the analysis one cannot usually determine to what extent the peak is composite. This image-point error remains as a slight error in the location of the corresponding atom. The error can only be removed by a subsequent refinement process.

Preliminary refinement

The structure of berthierite as found by image-seeking methods was believed to be essentially correct with regard to the general location of the atoms, since there was a rough agreement between computed and observed intensities. Nevertheless this agreement was not good. Refinement of this structure was evidently necessary. It was carried out in eleven stages. The migration of coordinates during the refinement is outlined in Table 1.

For the purpose of refining the structure, the observed $h\bar{k}0$ intensities were placed on an absolute basis using Wilson's (1942) method, Fig. 4. This analysis not only places the intensities on an absolute basis but also yields the temperature coefficient B . The value of this turned out to be 1.07 \AA^2 for berthierite. The value of B and the absolute scale of intensities were slightly improved when the structure was considerably refined.

The original structure as determined with the aid of the minimum function was termed trial 1. This was examined to ascertain what obvious shifts in atom locations would improve agreement between calculated and observed intensities. This predicted an improved set of atom locations which was called trial 2. This procedure was repeated, resulting in an improved set of atom locations called trial 3.

Further refinement

Residual factor. This marked the end of elementary methods of refining the structure. From this stage onward, the status of the refinement was followed by computing the observed and computed amplitude residual factor (Robertson and Woodward, 1936).

$$R = \frac{\sum |F_{\text{observed}}| - |F_{\text{calculated}}|}{|F_{\text{observed}}|}. \quad (1)$$

The magnitude of this factor varies somewhat depending upon how one treats the smallest F_0 and the smallest differences, $\Delta = F_0 - F_c$. In Table 2 we have computed four types of R , labelled (a), (b), (c), and (d). These are defined in Table 2.

Refinement by Patterson maps. The first non-elementary refinement procedure made use of comparing the weighted vector set of trial 3 with the observed Patterson map. These showed reasonably good agreement, but detailed comparison indicated that the agreement could be improved by some small shifts in the locations of some atoms. This improved structure was termed trial 5. Another set of atom locations, called trial 4, differs from trial 5 only in that the sulfur atoms had been moved to idealized covalent octahedral locations about iron. Table 1 shows that the residual factor for the ideal sulfur arrangement was so much worse that the possibility of an idealized FeS_6 group was evidently excluded.

From this point on the structure was refined chiefly by differential syntheses (Cochran, 1951), using as Fourier coefficients $(F_{\text{observed}} - F_{\text{computed}})_{hk0}$. This synthesis is known to minimize R .

First differential synthesis. The set of amplitudes F_c , computed from trial 5 (resulting from the refinement-by-Patterson procedure) was used to compute a differential synthesis, Fig. 6. The atom locations proved to be on gradients on this map, so the locations were shifted up-

gradient to produce a new set of locations, namely trial 6.

The change from trial 5 to trial 6 reduced the residual factor from 17.1% to 14.7%.

Electron density projection, $\rho(xy)$. At this point it was believed that the structure was in a sufficient state of refinement to warrant preparing an electron density projection, $\rho(xy)$. This is shown in Fig. 3. The peak locations of $\rho(xy)$ are taken as trial 7. Although the co-ordinates of trial 6 and trial 7 are different, they do not correspond to any changes in phase of F_{hkl} . Thus Fig. 3 may be taken as the final electron density map. The weighted vector set of trial 7 is shown superposed on the corresponding Patterson map in Fig. 1. The agreement between them is quite good, so that the structure may be said to neatly explain the Patterson synthesis.

In spite of the fact that Fig. 3 is the final $\rho(xy)$, the locations of its peaks do not provide the best values of the coordinates. This is obvious on studying Table 1. Trial 7 has a larger R value than trial 6. Furthermore, starting with trial 7, whose coordinates are derived from $\rho(xy)$, it is possible to obtain other sets of coordinates by refinement which have smaller R values, and without changing the phases of any F_{hkl} 's. That a set of F_{hkl} 's produces a map, $\rho(xy)$, whose peaks deviate slightly from the exact atom locations is due to using a finite set of F_{hkl} 's in the synthesis. This is the series-termination effect. This effect is substantially absent in differential

syntheses. The residual termination effect does not change the general course of the lines of the differential map, and consequently the gradient is insensitive to slight errors in the F 's. On the other hand the peak maximum in $\rho(xz)$ is, in general, shifted by the termination effect. The study given here presents detailed evidence that differential syntheses are superior to electron-density syntheses for refinement.

New scale factor. Up to this point the scale factor derived in Wilson's method had been used. Since no further sign changes were in prospect, the structure was regarded as sufficiently well-settled to permit computing a new refined scale factor, by plotting $\log \frac{F_o}{F_c}$ against $\sin^2\theta$. This is shown in Fig. 5. The change in the scale factor in going from Wilson's method to this method proved to be from 75.5 to 71.0, while B changed from 1.07 \AA^2 to 0.98 \AA^2 . The use of the new scale factor reduced the R factor from 15.8% to 14.2%.

Further refinement by differential synthesis. Trial 7 was further refined by a series of differential syntheses shown in Figs. 7, 8, 9, and 10. In these figures the atom locations used for the differential syntheses are shown as black dots. The criterion for correct atom position is that the original atom locations are found to lie on positions of zero gradient on the differential map. In each trial, therefore, the dots were moved up-gradient in the hope that the subsequent synthesis would show them to lie on zero gradient.

In order to find the parameter range within which the Sb's must lie, these were moved by .005 from trial 7 to trial 8. This move proved to be too much, as indicated by the sharp reversal of gradient which accompanied the shift. Subsequent trials have Sb parameters between the values used for trial 7 and trial 8.

The Fe and three of the S atoms assumed positions of substantially zero gradient by trial 9. In trial 10 the other atoms are also in zero-gradient position but the Fe atom again appears to lie on a slight gradient. This is probably due to contributions from other atoms and therefore signifies that refinement of the Fe position has been achieved within the accuracy of our data. Trial 11 was devised to give the Fe and 2 S's a slight shift to improve their positions on gradients. This last set of shifts produced a set of parameters having higher R values. Trial 10 was accordingly accepted as the final set of parameters since all the atoms are all on substantially zero gradient even though its R value is slightly greater than that of trial 9.

After computing this set of differential syntheses, it became evident that a shift of parameters of .001 or .002 changes the configuration of the map strongly and in such a way as to reverse the gradient, at least for the heavier atoms when they are in the neighborhood of the correct locations. From this it is deduced that the accuracy of the final atomic coordinates given for berthierite is about .002, which is equivalent to about $.02\text{\AA}$. It is of interest to note that

when the atoms are in the neighborhood of their final correct positions the major features of the differential map coincide with the background of the electron density map. The features of the differential map must, therefore, be regarded as due chiefly to errors in the determination of the F_o 's.

Selection of z parameters

The xy coordinates of all atoms in the structure are now known with accuracy. Since the atoms are confined to the reflection planes, their coordinates can be either $\frac{1}{4}$ or $-\frac{1}{4}$. The only combination which was acceptable was found by making a limited number of intensity computations for $F_{\underline{h}01}$. A complete set of $F_{\underline{h}01}$'s was computed based upon this combination. These were independently placed on an absolute basis by comparing observed and computed intensities. The resulting temperature factor, B, for the h01 reflections proved to be 0.99, compared with 0.98 found previously for the hk0 reflections. The resulting R values are shown in Table 3. The electron-density projection $f(\underline{xz})$ is shown in Fig. 11. In this projection some of the atoms are unresolved due to overlapping.

The final structure

The electron density projections for the entire cell

are shown in proper relation in Fig. 12. The final parameters are given in Table 4. A comparison of observed and computed F values is given in Tables 5 and 6.

Discussion of the structure

The distances between neighboring atoms in berthierite are listed in Table 7. These distances are shown in a diagrammatic representation of the structure in Fig. 13.

It is convenient to discuss the structure of berthierite in two stages. In the first stage account is taken only of the nearest neighbors. Table 7 and Fig. 13 show that each of the two kinds of Sb atoms has three nearest S neighbors at distances of about 2.5°A , as well as other S atoms at larger distances. The Sb and S atoms thus form SbS_3 groups. Each group shares two of its three S atoms with translation-equivalent groups to form SbS_2 chains parallel to the c axis.

The Fe atoms are surrounded by six S atoms in approximately octohedral arrangement. These octohedra share edges to form chains parallel to the c axis. The Fe-S distance is about 2.5°A . This is considerably in excess of that found in structures where the bonds are recognized as covalent (pyrite, 2.26°A , marcasite, 2.24°A). The distance is about what would be expected for ionic Fe-S bonds. Thus, the structure of berthierite suggests that its chemical nature is $\text{Fe}^{++}(\text{SbS}_2)_2^-$. Curiously enough, the Sb_I triangles share an

edge with each of two neighboring Fe octohedra, whereas the Sb_{II} triangles only share corners with these octohedra.

Each of the four kinds of sulfur atoms in berthierite is coordinated to three metal atoms and each such set of metals contains both Fe and Sb atoms.

If one takes account of second nearest interatomic distances then it becomes evident that the two kinds of Sb atoms are quite different. The Sb_{II} has no further neighbors nearer than 3.2 \AA while Sb_I has two additional neighbors at about 2.9 \AA . This rather close distance doubtless represents a bond, so that one can also describe the Sb_I atoms as forming irregular SbS₅ groups. Two such SbS₅ groups, related by the inversion center in the middle of Fig. 13, share the two second-nearest S's with each other so that a complex chain of composition Sb₂S₄ can be discerned parallel to the c axis. An alternative description is that the two SbS₂ chains, related by the inversion center in the middle of Fig. 13, can be regarded as joined so as to form more complex chains of composition Sb₂S₄. This kind of double chain has also been discovered in livingstonite (Buerger and Niizeki, 1954). The two kinds of sulfur coordination displayed by Sb_{II} and Sb_I atoms are also found in the two types of Sb atoms of stibnite.

The Fe atom appears to have the function of cementing together the two kinds of SbS₂ chains. It should be noted that the coordination of Fe is irregular octohedral. Four of the S atoms are at distances of about 2.46 \AA but two more are

at distances of 2.64\AA . This condition is quite real since an attempt to regularize the distances resulted in a much higher R value.

The cleavage of berthierite is reported in one reference as more or less distinct parallel to one pinacoid, and in another reference as rather distinct prismatic. Fig. 13 shows that a cleavage could occur parallel to (010) without the breaking of any bonds except the 2.93\AA bond from Sb_{II} to Si_{IV}.

Acknowledgement

This research was supported by the Office of Naval Research under Contract No. N5ori-07860 with the Massachusetts Institute of Technology.

References

- Buerger, M.J. (1936). Amer. Mineral. 21, 442-448.
- Buerger, M.J. (1950). Proc. Nat. Acad. Sci. 36, 738-742.
- Buerger, M.J. (1951). Acta Cryst. 4, 531-544.
- Buerger, M.J. and Niizeki, Nobukazu. (1954). Amer. Mineral. 39.
- Cochran, W. (1951). Acta Cryst. 4, 81-92.
- Dawton, Ralph H.V.M. (1938). Proc. Phys. Soc. 50, 919-925.
- Robertson, J. Monteath and Woodward, Ida. (1936). J. Chem. Soc. Lond., 1817-1824, esp. p. 1822.
- Wilson, A.J.C. (1942). Nature. 150, 152.
- Zsivny, Victor and Zombory, László. (1934). Mineral. Mag. 23, 566-568.

Table 1
Coordinates of Atoms for Different Trials

		Trial										
		1	2	3	4	5	6	7	8	9	10	11
Sb _I	x	.147	.148	.149	.149	.149	.148	.145	.140	.143	.145	.145
	y	.060	.059	.059	.063	.063	.063	.064	.063	.063	.062	.062
Sb _{II}	x	.040	.044	.041	.037	.037	.038	.036	.041	.039	.037	.037
	y	.384	.382	.381	.387	.387	.386	.385	.386	.386	.386	.386
Fe	x	.321	.318	.318	.323	.323	.321	.314	.320	.316	.316	.317
	y	.340	.336	.337	.339	.339	.337	.335	.335	.334	.334	.335
S _I	x	.190	.204	.200	.230	.200	.200	.197	.197	.196	.195	.194
	y	.270	.273	.273	.290	.273	.270	.272	.272	.272	.272	.272
S _{II}	x	.414	.419	.421	.417	.421	.424	.428	.428	.426	.424	.423
	y	.200	.186	.187	.198	.187	.185	.186	.186	.185	.184	.185
S _{III}	x	.240	.229	.230	.237	.230	.227	.229	.229	.227	.226	.226
	y	.485	.495	.494	.484	.494	.493	.494	.494	.492	.492	.492
S _{IV}	x	.452	.452	.450	.418	.450	.451	.452	.452	.450	.451	.451
	y	.408	.407	.407	.388	.407	.404	.405	.405	.406	.405	.405

Table 2
R Factors for F_{hkl} for Different Trials

		3	4	5	6	7	8	9	10	11
R.%	(a)	19.0	27.3	17.1	14.7	15.8				
						14.2*	14.3*	12.4*	12.8*	13.2*
	(b)	17.8	26.4	16.0	12.6	13.2				
						12.3*	12.2*	10.2*	10.8*	11.1*
(c)		24.5	38.5	22.5	19.1	19.8				
						18.6*	19.3*	16.8*	17.1*	17.3*
(d)		23.3	37.4	19.8	17.2	17.6				
						16.8*	17.2*	14.7*	15.1*	15.3*

(a) $\Delta F = \underline{F}_0 - \underline{F}_0$ omitted if $\underline{F}_0 = 0$.

(b) $\Delta F = \underline{F}_0 - \underline{F}_0$ omitted if $\Delta <$ least significant difference.

(c) When $\underline{F}_0 = 0$, it is assigned a mean value between true zero and least observable \underline{F}_0 .

(d) Condition b and c together.

* New scale.

Table 3
R Factors for \bar{E}_{h01}

(a)	8.8%
(b)	5.9%
(c)	8.8%
(d)	5.9%

(See Table 2 for explanation of conditions a, b, c, and d.)

Table 4
Final Coordinates of Atoms in Berthierite

	x	y	z
Sb _I	0.145	0.062	+0.250
Sb _{II}	0.037	0.386	-0.250
Fe	0.316	0.334	+0.250
S _I	0.195	0.272	-0.250
S _{II}	0.424	0.184	+0.250
S _{III}	0.226	0.492	+0.250
S _{IV}	0.451	0.405	-0.250

Table 5 (Page 1)

Observed and Calculated Structure Factors for hk0-zone

hk0	F _{obs}	F _{calc}	hk0	F _{obs}	F _{calc}	hk0	F _{obs}	F _{calc}
020	71	+100	1,12,0	78	+ 75	2,12,0	92	- 86
040	128	-158	1,13,0	135	+122	2,13,0	135	+124
060	85	- 87	1,14,0	135	+112	2,14,0	121	-103
080	<52	- 33	1,15,0	<70	+ 33	2,15,0	<70	+ 44
0,10,0	<58	+ 26	1,16,0	<71	- 34	2,16,0	<71	+ 14
0,12,0	<64	+ 17	1,17,0	<70	- 44	2,17,0	<70	- 22
0,14,0	<69	- 34	1,18,0	<68	- 20	2,18,0	<67	- 2
0,16,0	99	+ 87	1,19,0	<62	+ 11	2,19,0	99	- 74
0,18,0	178	+140	200	42	+ 40	310	281	-240
110	<23	+ 1	210	42	- 41	320	<41	+ 27
120	<25	+ 30	220	<29	+ 4	330	114	+ 88
130	121	+132	230	185	-178	340	57	+ 53
140	149	-172	240	213	-213	350	128	+132
150	<41	+ 30	250	185	-194	360	178	-176
160	92	- 96	260	92	- 98	370	<52	+ 31
170	106	-109	270	71	+ 64	380	78	- 86
180	<52	+ 1	280	71	+ 39	390	114	+110
190	164	-186	290	<56	- 11	3,10,0	35	+ 85
1,10,0	85	+ 91	2,10,0	99	+110	3,11,0	<63	+ 19
1,11,0	<61	- 8	2,11,0	<58	+ 18	3,12,0	78	+ 72

Table 5 (Page 2)

hk0	F _{obs}	F _{calc}	hk0	F _{obs}	F _{calc}	hk0	F _{obs}	F _{calc}
3,13,0	<63	+ 49	4,17,0	<68	+ 49	620	<56	+ 25
3,14,0	<69	- 14	4,18,0	<64	+ 3	630	<56	+ 31
3,15,0	<70	- 35	4,19,0	<50	- 26	640	<57	- 40
3,16,0	<71	- 30	510	<51	- 55	650	99	+ 77
3,17,0	106	-107	520	263	+225	660	57	- 64
3,18,0	<55	- 43	530	106	- 71	670	135	+151
3,19,0	35	- 52	540	277	+252	680	<62	- 57
400	<46	- 7	550	<55	+ 56	690	78	- 82
410	<46	- 18	560	<56	- 40	6,10,0	78	- 87
420	<47	- 40	570	<58	+ 27	6,11,0	149	-166
430	64	- 43	580	92	- 92	6,12,0	<69	- 3
440	<50	- 54	590	99	-120	6,13,0	<70	- 27
450	192	+189	5,10,0	<64	+ 33	6,14,0	<70	+ 24
460	<54	+ 46	5,11,0	<66	+ 51	6,15,0	<70	+ 31
470	<56	+ 64	5,12,0	<68	- 10	6,16,0	<68	+ 15
480	173	+199	5,13,0	<69	+ 1	6,17,0	<65	+ 16
490	42	- 62	5,14,0	85	- 78	6,18,0	78	+ 60
4,10,0	106	+127	5,15,0	<70	- 23	710	149	+142
4,11,0	<65	- 64	5,16,0	<70	- 33	720	220	+194
4,12,0	<67	- 18	5,17,0	<67	- 31	730	<59	+ 50
4,13,0	<68	- 40	5,18,0	<62	+ 38	740	<61	- 26
4,14,0	85	- 66	600	128	+119	750	<62	+ 26
4,15,0	<70	+ 45	610	<55	- 21	760	99	-101
4,16,0	<70	- 42				770	78	- 88

Table 5 (Page 3)

hk0	F _{obs}	F _{calc}	hk0	F _{obs}	F _{calc}	hk0	F _{obs}	F _{calc}
780	<65	- 56	8,14,0	85	+ 68	10,5,0	<68	+ 41
790	<66	- 58	8,15,0	120	+105	10,6,0	92	+104
7,10,0	<67	- 41	8,16,0	153	+ 48	10,7,0	<68	- 12
7,11,0	<58	- 27	910	<65	- 49	10,8,0	<69	+ 25
7,12,0	<70	+ 59	920	<66	- 6	10,9,0	<69	+ 6
7,13,0	<70	+ 27	930	<66	- 45	10,10,0	<69	- 12
7,14,0	<70	+ 9	940	<66	- 39	10,11,0	<68	- 19
7,15,0	85	+ 73	950	<67	- 35	10,12,0	<67	+ 35
7,16,0	92	- 91	960	114	-140	10,13,0	<66	- 25
7,17,0	99	+ 82	970	<68	+ 17	10,14,0	<62	0
800	106	- 84	980	<68	- 50	10,15,0	<52	+ 50
810	106	- 92	990	<68	- 50	11,1,0	<68	+ 5
820	99	+106	9,10,0	85	+ 90	11,2,0	64	+ 98
830	156	-153	9,11,0	<66	- 23	11,3,0	64	- 60
840	64	+ 59	9,12,0	120	+151	11,4,0	<68	+ 23
850	<64	- 21	9,13,0	99	- 69	11,5,0	<68	+ 3
860	<65	- 41	9,14,0	<66	- 21	11,6,0	<68	+ 16
870	<66	+ 35	9,15,0	<62	- 8	11,7,0	120	+133
880	<67	- 37	9,16,0	<51	- 15	11,8,0	<68	- 21
890	<68	+ 25	10,0,0	149	-131	11,9,0	64	+ 59
8,10,0	<68	- 42	10,1,0	121	-100	11,10,0	<68	+ 2
8,11,0	<69	- 8	10,2,0	121	-115	11,11,0	<66	+ 25
8,12,0	<69	- 25	10,3,0	64	- 84	11,12,0	<63	- 11
8,13,0	71	+ 65	10,4,0	92	+ 81	11,13,0	<60	- 43

Table 5 (Page 4)

hk0	F _{obs}	F _{calc}	hk0	F _{obs}	F _{calc}	hk0	F _{obs}	F _{calc}
11,14,0	<50	- 33	13,1,0	<68	+ 58	14,4,0	64	+ 83
12,0,0	99	- 84	13,2,0	<68	+ 44	14,5,0	<61	0
12,1,0	<68	+ 8	13,3,0	<67	+ 2	14,6,0	<59	- 14
12,2,0	<68	- 30	13,4,0	<67	+ 21	14,7,0	<58	- 16
12,3,0	<68	+ 59	13,5,0	85	- 98	14,8,0	71	- 99
12,4,0	<68	+ 60	13,6,0	<66	+ 25	14,9,0	<42	+ 9
12,5,0	<68	+ 47	13,7,0	<65	- 53	15,1,0	57	+ 71
12,6,0	64	+ 67	13,8,0	<63	+ 24	15,2,0	92	- 100
12,7,0	64	+ 89	13,9,0	<60	+ 39	15,3,0	<55	+ 4
12,8,0	64	- 76	13,10,0	<55	- 36	15,4,0	<53	- 29
12,9,0	<66	- 9	13,11,0	71	- 71	15,5,0	<50	- 59
12,10,0	<64	- 45	14,0,0	<65	- 10	15,6,0	<33	- 20
12,11,0	57	-106	14,1,0	<65	+ 2	16,0,0	<40	- 40
12,12,0	<55	+ 35	14,2,0	<64	+ 46	16,1,0	<45	- 9
12,13,0	<32	- 34	14,3,0	<63	- 38	16,2,0	71	- 51

Table 6
Observed and Calculated Structure Factors for h01-zone

$h01$	F_{obs}	F_{calc}	$h01$	F_{obs}	F_{calc}
002	492	-470	800	100	- 85
004	280	+269	801	<63	- 2
200	36	+ 40	802	80	+ 71
201	<40	- 1	803	<70	+ 1
202	<52	- 33	804	52	- 45
203	<63	- 3	10,0,0	120	-135
204	<70	+ 20	10,0,1	48	+ 51
205	<63	+ 3	10,0,2	104	+115
400	<46	- 9	10,0,3	<69	- 37
401	104	-105	10,0,4	72	- 77
402	<55	+ 5	12,0,0	92	- 85
403	68	+ 79	12,0,1	144	-167
404	<70	- 1	12,0,2	72	+ 73
405	48	- 40	12,0,3	116	+129
600	108	+121	14,0,0	<65	- 6
601	244	-236	14,0,1	<64	+ 39
602	80	- 94	14,0,2	<68	+ 5
603	148	+159	16,0,0	<40	- 41
604	48	+ 58			

Table 7
Interatomic Distances in Berthierite

	S_I	S_{II}	S_{III}	S_{IV}
Sb_I	3.56 (2)	3.63 (1)	2.58 (2)	{ 2.48 (1) 2.93 (2)
Sb_{II}	2.43 (1)	2.48 (2)	{ 3.24 (2) 3.47 (1)	
Fe	2.49 (2)	2.45 (1)	2.46 (1)	2.64 (2)
S_I	3.76 (2)	3.45 (2)	3.64 (2)	
S_{II}		3.76 (2)		3.66 (2)
S_{III}			3.76 (2)	3.43 (2)
S_{IV}				3.76 (2)

Note: Numbers in parentheses indicate the number of distinct vectors of this length.

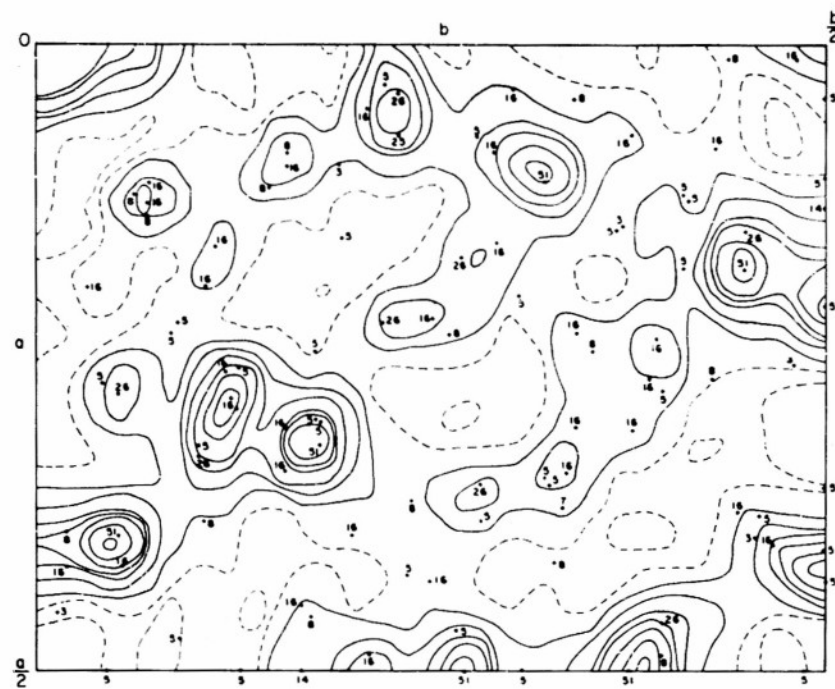


Fig. 1

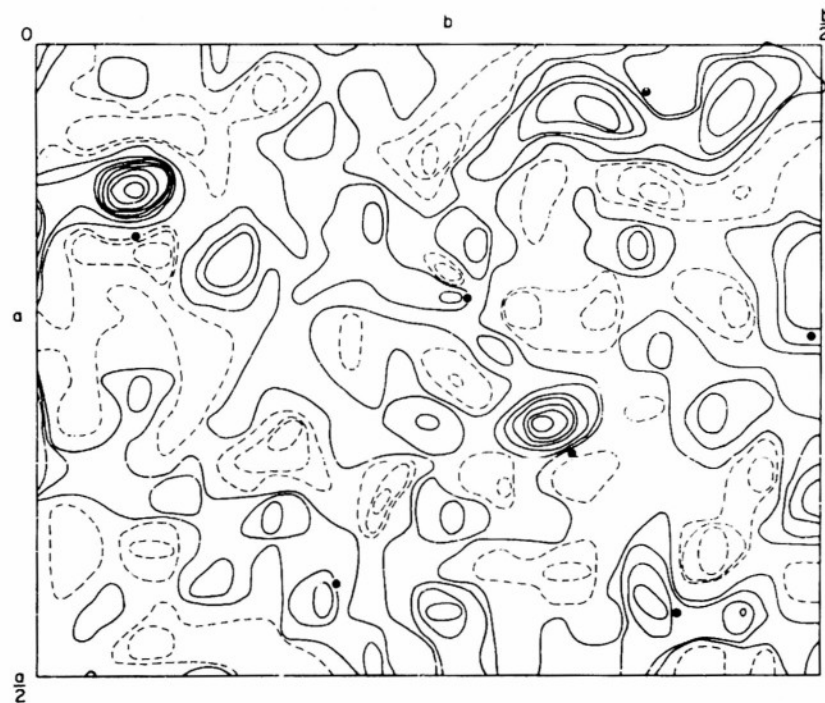


Fig. 6

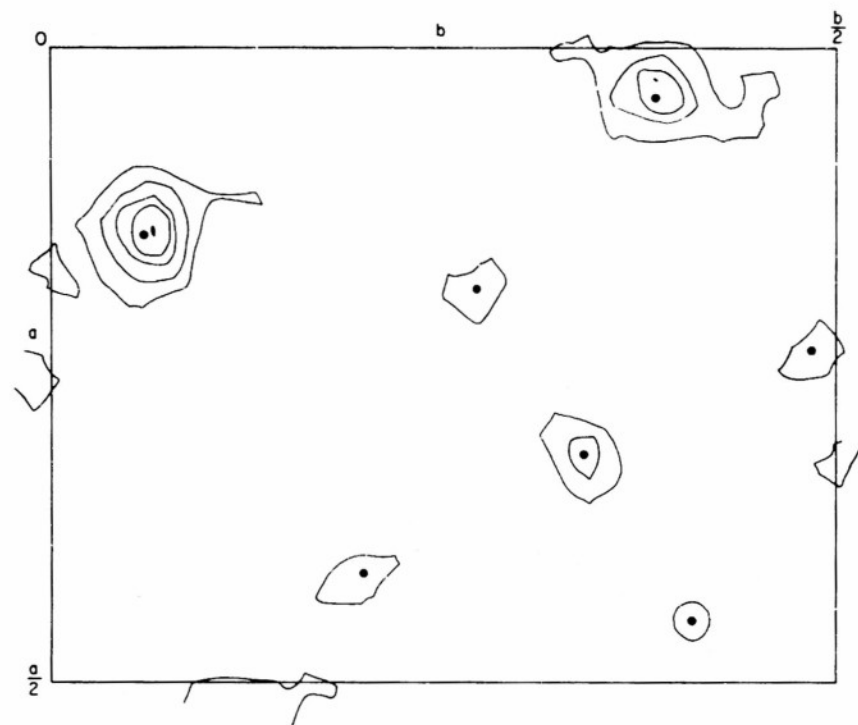


Fig. 2

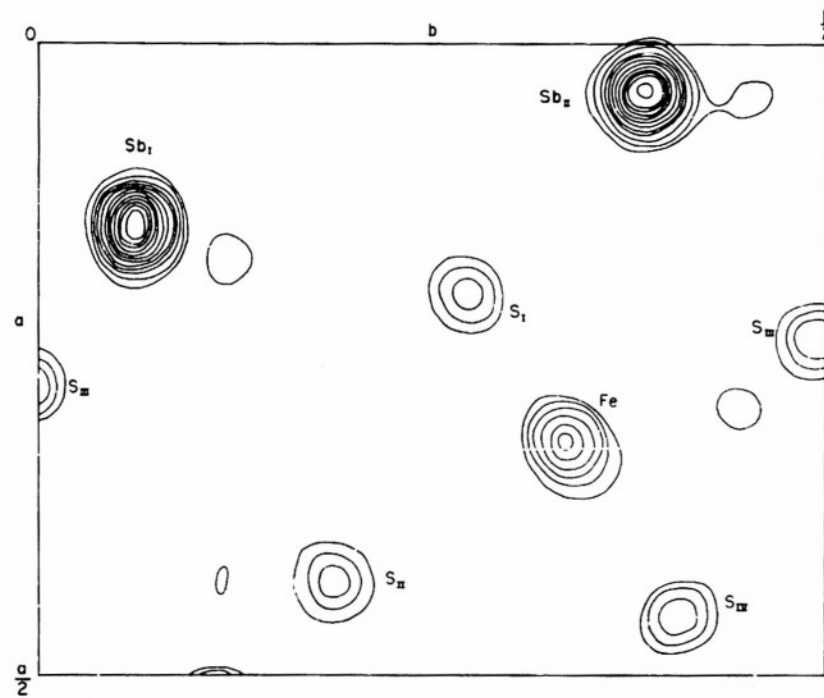


Fig. 3

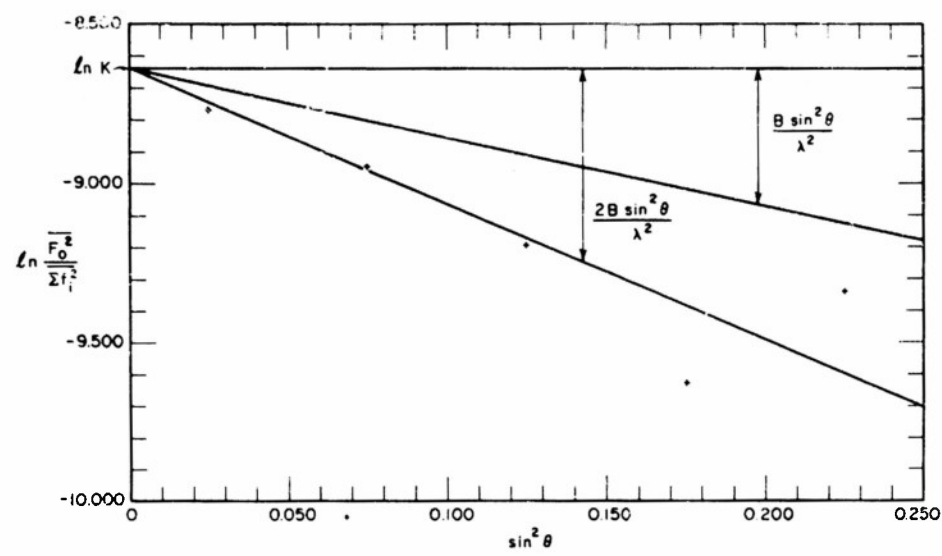


Fig. 4

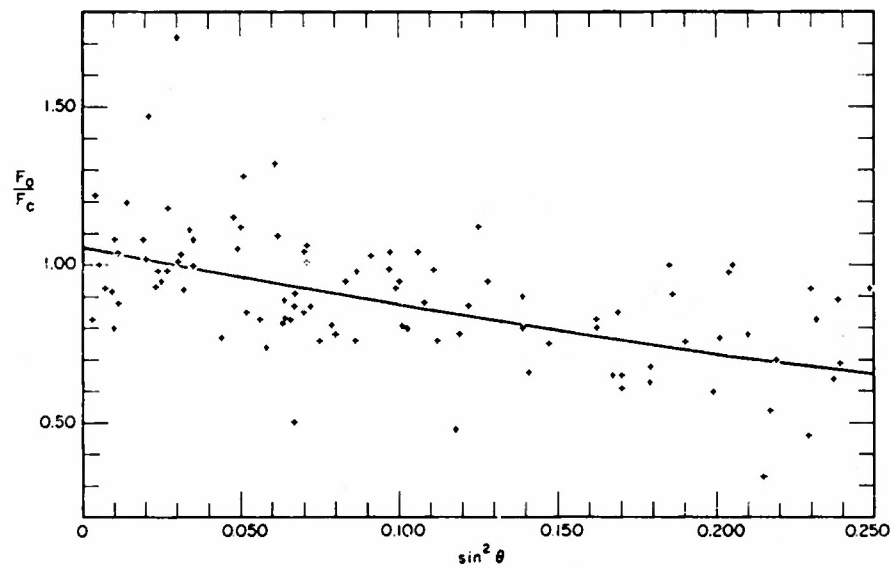


Fig. 5A

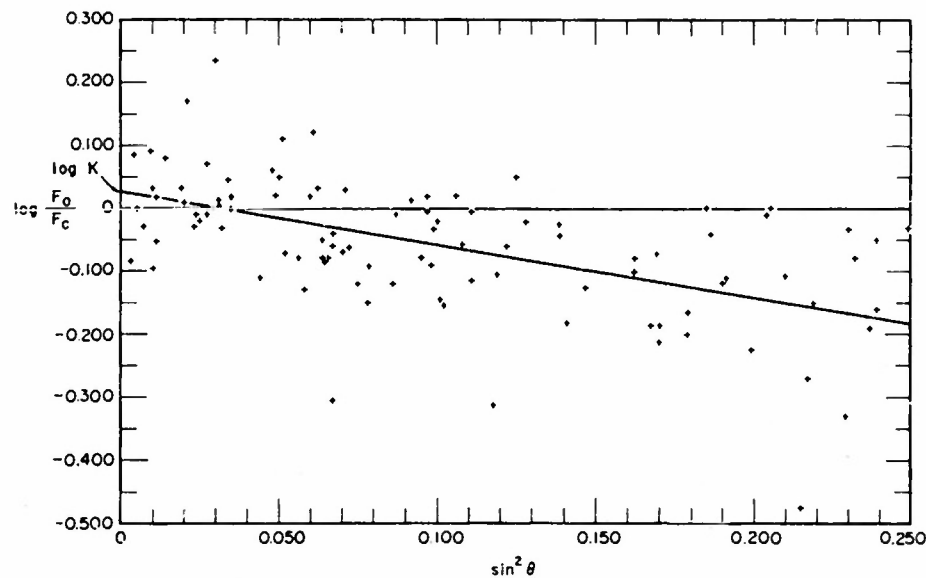


Fig. 5B

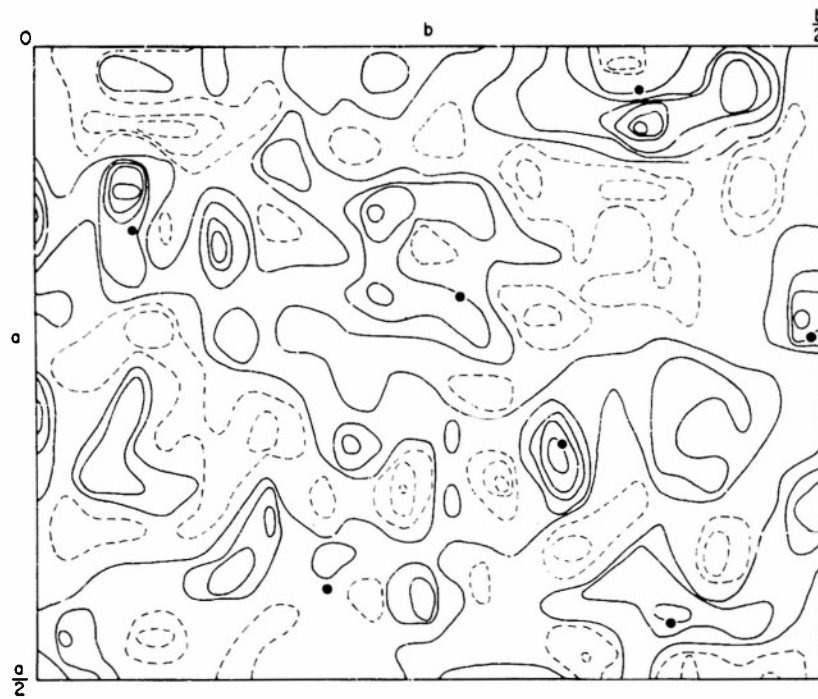


Fig. 7

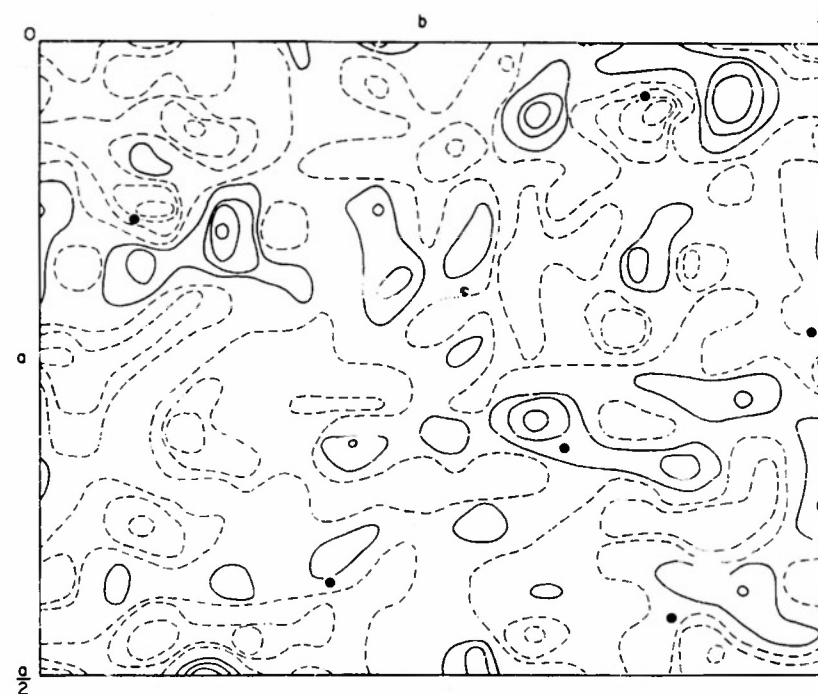


Fig. 8

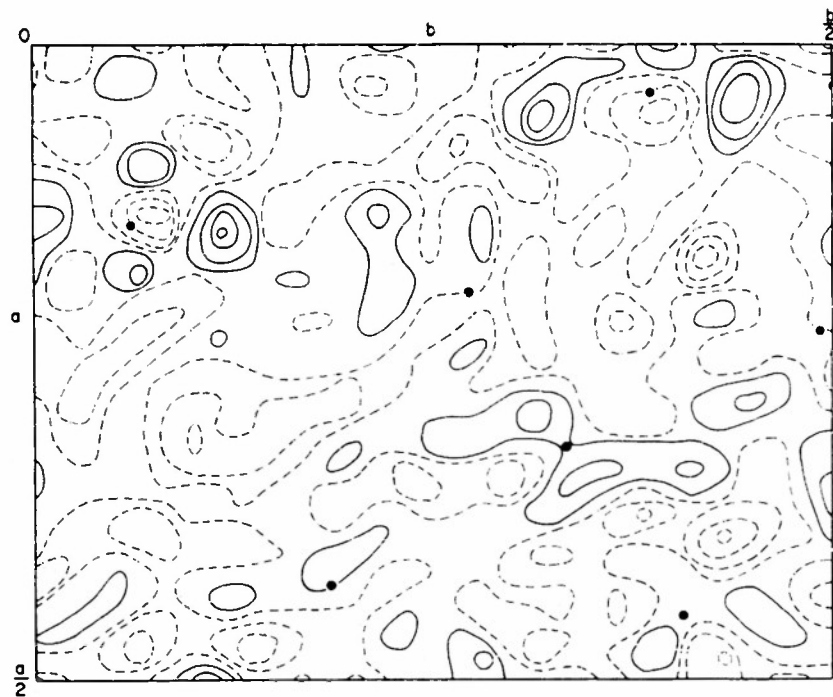


Fig. 9

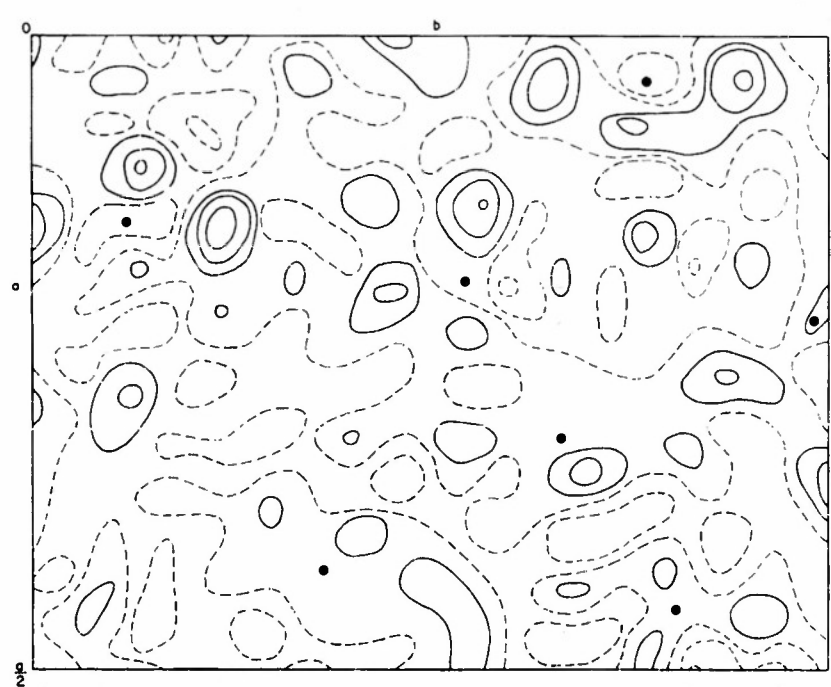
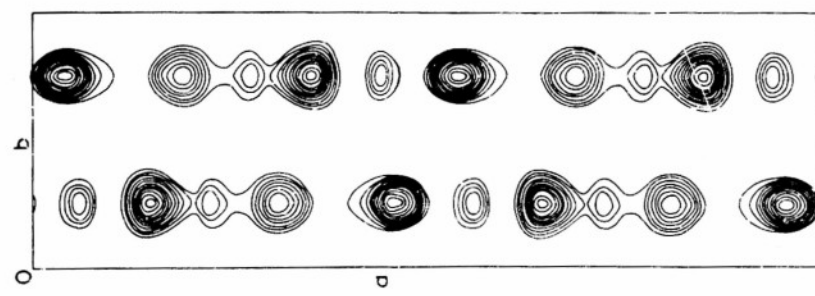
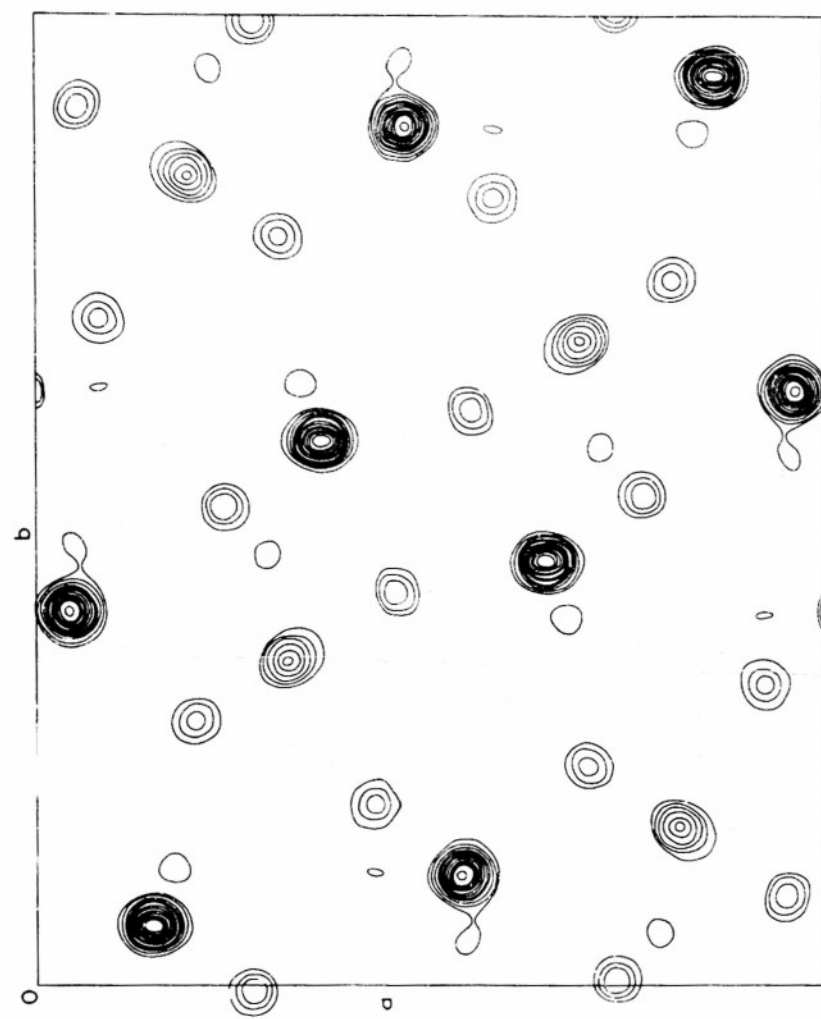


Fig. 10

FIG. 12



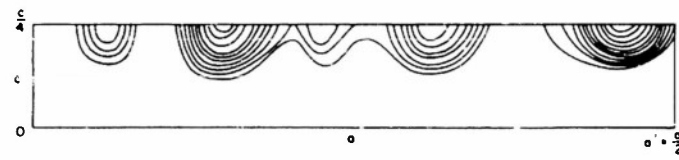


Fig. 11

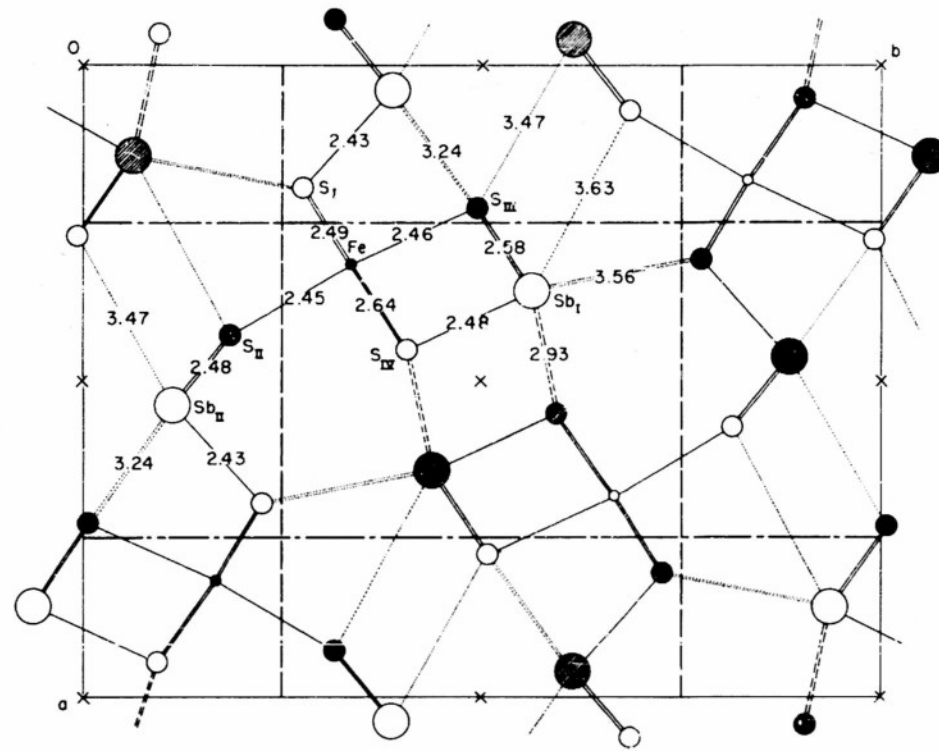


Fig. 13